Atmos. Chem. Phys. Discuss., 8, 18911–18936, 2008
www.atmos-chem-phys-discuss.net/8/18911/2008/

Atmospheric Chemistry and Physics Discussions

This discussion paper is/has been under review for the journal *Atmospheric Chemistry and Physics (ACP)*. Please refer to the corresponding final paper in *ACP* if available.

Anthropogenic influence on SOA and the resulting radiative forcing

C. R. Hoyle[1,3], G. Myhre[2], T. K. Berntsen[1,2], and I. S. A. Isaksen[1]

[1]Department of Geosciences, University of Oslo, Norway
[2]Center for International Climate and Environmental Research, Oslo, Norway
[3]Institute for Atmospheric and Climate Science, ETH Zurich, Zurich, Switzerland

Received: 11 September 2008 – Accepted: 17 September 2008 – Published: 3 November 2008

Correspondence to: C. R. Hoyle (c.r.hoyle@geo.uio.no)

Published by Copernicus Publications on behalf of the European Geosciences Union.

Abstract

The pre-industrial and present day distributions and burdens of Secondary Organic Aerosol (SOA) have been calculated using the off-line aerosol chemistry transport model Oslo CTM2. The production of SOA was found to have increased from about 43 Tg yr^{-1} to 69 Tg yr^{-1} since pre-industrial times, leading to an increase in the global annual mean SOA burden from 0.44 Tg to 0.70 Tg, or about 59%. The increases are greatest over industrialised areas, as well as over regions with high biogenic precursor emissions. The contribution of emissions from different sources to the larger SOA burdens has been calculated. The results suggest that the majority of the increase is caused by emissions of primary organic aerosols (POA), from fossil fuel and bio fuel combustion. When SOA partitioning to ammonium sulphate aerosol was not accounted for, the increase in SOA burden between pre-industrial times and the present was found to be lower (51%), with a production increase of 55%. As yet, very few radiative forcing estimates of SOA exist, and no such estimates were provided in the latest IPCC report. In this study, we find that the change in SOA burden caused a radiative forcing of -0.09 W m^{-2}, when SOA was allowed to partition to both organic and sulphate aerosols, and -0.06 W m^{-2} when only partitioning to organic aerosols was assumed. Therefore, the radiative forcing of SOA is found to be substantially stronger than the best estimate for POA in the latest IPCC assessment.

1 Introduction

Atmospheric aerosols play a key role in determining the Earth's radiation budget (IPCC, 2007; Schulz et al., 2006; Kaufman et al., 2002). Secondary organic aerosol (SOA) represents an important, and under certain circumstances, the major, fraction of the global organic aerosol (OA, i.e. SOA + POA) burden (Kanakidou et al., 2005).

There has been considerable change to the composition and magnitude of emissions from anthropogenic activities since pre-industrial times, therefore it is important

ACPD

8, 18911–18936, 2008

to investigate how these changes have influenced the distribution and global burden of organic aerosols.

The change in SOA production and burden since pre-industrial times was first examined with a global model by Kanakidou et al. (2000), who considered SOA formation only from the oxidation products of the reaction of α- and β-pinene with ozone. Subsequent studies involved a range of monoterpenes and other reactive volatile organic compounds (ORVOC), but used prescribed oxidant fields (Chung and Seinfeld, 2002), or did not include SOA formation from the oxidation products of isoprene, or anthropogenic SOA precursors (Liao and Seinfeld, 2005). A recent study by Tsigaridis et al. (2006) used α- and β-pinene to represent biogenic SOA precursors, and toluene and xylene to represent the anthropogenic SOA precursors, however SOA formation from isoprene oxidation was taken into account using a 0.2% aerosol molar yield, leading to a far lower contribution of isoprene to present day SOA burdens than that found by Henze and Seinfeld (2006). In the present study we calculated the change in SOA production, burden and radiative forcing since the pre-industrial times, accounting for SOA formation from four classes of monoterpene as well as sesquiterpenes, ORVOC, benzene, toluene, xylene, trimethylbenzene and isoprene. Oxidation of these precursors was calculated with a comprehensive global tropospheric chemistry scheme.

By performing several model integrations, including emissions from different sources, the contribution of increases in biomass burning POA to the total increase in SOA was separated from the increase due to the anthropogenic influence on gas phase atmospheric chemistry, and direct emissions of organic aerosols from fossil and bio fuel burning.

In Sect. 2, the chemistry transport model (CTM), the SOA scheme and the details of the model experiments are described. The radiative transfer model used to calculate the radiative forcing of the change in SOA burden is described in Sect. 3, and the results are presented in Sect. 4. Section 5 provides a summary and discussion.

ACPD
8, 18911–18936, 2008

2 The Oslo CTM2

The Oslo CTM2 is a three-dimensional off-line chemistry transport model, which was run in T42 (approximately 2.8°× 2.8°) resolution for this study. The meteorological data used was generated by running the Integrated Forecast System (IFS) of the European Centre for Medium Range Weather Forecasts (ECMWF), for the year 2004, and was updated (off-line) in the CTM every three hours. The same meteorological data was used for both the present day and the pre-industrial simulations.

The model is divided into 40 layers between the surface and 10 hPa. The chemical time step in the troposphere was 15 min, and the transport time step was based on the CFL criteria. In the free troposphere the greatest possible transport time step was one hour and in the boundary layer it was 15 minutes.

In the configuration used for the present day simulation, the model included 122 gas and condensed phase chemical species, all of which were transported. The chemistry scheme accounted for the most important parts of the ozone-NO_x-hydrocarbon chemistry cycle. For the chemistry calculations, the QSSA chemistry solver (Hesstvedt et al., 1978) was used. More detailed descriptions of the model can be found in Berglen et al. (2004) and Berntsen and Isaksen (1997).

The SOA module which has recently been added to the Oslo CTM2 accounts for SOA formation from the oxidation products of biogenically emitted volatile organic compounds (predominantly monoterpenes and isoprene) as well as benzene, toluene, xylene, and other aromatic compounds. Volatile hydrocarbons were emitted in the lowest layer of the model and oxidised in the gas phase by OH, O_3 and NO_3, to give semi-volatile oxidation products according to a two-product model (Odum et al., 1996). These products were allowed to partition to existing organic aerosol (also to ammonium sulphate aerosol in some experiments) with the partitioning between gas and aerosol phase being calculated using empirically determined partitioning coefficients. The gas and aerosol phase oxidation products as well as the precursor VOC were subject to wet deposition in both convective and large scale rain. Additionally, the aerosol phase

ACPD
8, 18911–18936, 2008

species in the lowest model layer had a dry deposition loss term applied. A full description, as well as a validation of the SOA scheme against surface measurements is given in Hoyle et al. (2007). Model runs with and without SOA partitioning to sulphate aerosol were considered in Hoyle et al. (2007), for the present day, and it was found that allowing partitioning to sulphate aerosol improved the comparison with measurements substantially. In the present work, these runs are therefore our main focus.

2.1 Experiments

Six model experiments were carried out to investigate the change in SOA production and burden since pre-industrial times, as listed in Table 1. The first two experiments (Pind_std and Pres_std) were run for the years 1750 and 2004, respectively. In these experiments the primary organic aerosol, which was available for the SOA to partition to, was emitted via fossil fuel, bio fuel and biomass combustion. SOA was also assumed to partition to ammonium sulphate aerosol.

Run Pres_BBpind was identical to Pres_std except that POA and sulphur emissions from biomass burning were set to 1750s levels. Similarly, Pind_BBpres was a run with 1750s emissions, except for biomass burning emissions of POA and sulphur, which were set to 2004 levels. It is important to note that in the latter two runs, the only components of biomass burning which were changed were the POA and SO_2/SO_4 emissions, the other biomass burning components were as for the base year (2004 and 1750, respectively). The runs were designed in this way to permit extraction of the effect of increasing aerosol available for partitioning, due to increases in biomass burning as a result of anthropogenic activity.

Finally, a present day and pre-industrial model run were carried out including SOA partitioning to POA from biomass, fossil fuel and bio fuel burning, but not including SOA partitioning to ammonium sulphate aerosol (Pres_nosul and Pind_nosul, respectively).

For all model runs, the meteorological data for 2004 was used. The emissions used in the present day and pre-industrial runs are described in Sect. 2.2. Using the first four model runs, it is possible to examine the changes in SOA production and burden since

ACPD
8, 18911–18936, 2008

pre-industrial times, as well as to separate the contributions of increases in POA from biomass burning and fuel burning or industrial emissions to the SOA burden. Runs Pres_nosul and Pind_nosul help characterise the effects of increases in ammonium sulphate aerosol since pre-industrial times.

2.2 Emissions

The biogenic emissions used for the present day and the pre-industrial runs were identical, as changes since pre-industrial times are expected to be only 2–3% (Lathière et al., 2005). Keeping the biogenic emissions constant had the added advantage of facilitating the calculation of the change in SOA directly related to anthropogenic emissions changes. Biogenic emissions of monoterpenes, isoprene and ORVOC were taken from the Global Emissions Inventory Activity (GEIA) data base and are representative of 1990 (Guenther et al., 1995). Isoprene emissions were reduced so that the annual global emissions were 220 $Tg\,yr^{-1}$ (IPCC, 2001). This is lower than recent estimates of isoprene emissions (460–570 $Tg\,yr^{-1}$ (Lathière et al., 2006), 500–750 $Tg\,yr^{-1}$ (Guenther et al., 2006) and 374–449 $Tg\,yr^{-1}$ Muller et al., 2008), therefore the amount of SOA formed from oxidation products of isoprene may be underestimated. Since isoprene emission estimates larger than those given in IPCC (2001) have appeared, there has been a discrepancy between these estimates and the magnitude of isoprene emissions suggested by global model studies. Increasing the isoprene emissions in global models has the effect of depleting OH concentrations, and this depletion could only be balanced by far too large O_3 concentrations. Recent work by Lelieveld et al. (2008) however, has suggested a mechanism by which OH consumed in isoprene oxidation may be recycled, which, if confirmed, would permit larger isoprene emissions in global models.

For the present day simulation, emissions of CO, NO_x and non-methane hydrocarbons were taken from the Precursors of Ozone and their Effects in the Troposphere (POET) inventory (Granier et al., 2005). Methane mixing ratios were fixed at 1750 ppbv at the surface for the present day simulations. Emissions of POA from biomass burn-

ACPD
8, 18911–18936, 2008

ing were taken from the Global Fire Emissions Database version 2 (GFEDv2), for 2004 (van der Werf et al., 2006), and POA emissions from fossil fuel and bio fuel combustion were from the inventory of Bond et al. (2004).

The pre-industrial emissions of POA from biomass burning and from bio fuel burning were from the AeroCom (Aerosol Inter-Comparison project) emissions datasets (Dentener et al., 2006). In the pre-industrial experiments, all fossil fuel related and industrial emissions were set to zero, and annual emissions of non-POA species emitted via biomass burning (for example SO_2, CO, NO_x and NMHC) were scaled down. This scaling was achieved by dividing the POA emissions for 1750 by the average POA emissions for 2000–2004, in order to generate monthly mean scaling factors for each point on the model grid at the surface. The resulting annual and global mean reduction in each type of emissions in the pre-industrial runs was 65%. This method implicitly assumes that biomass burning emissions of all the scaled species are proportional to changes in emissions of POA, however, given the large uncertainty in pre-industrial biomass burning emissions, this approach is justified. Methane mixing ratios at the surface were fixed at 700 ppb. The emissions used in each of the model experiments are summarised in Table 2.

3 The radiative transfer model

The radiative forcing of the SOA was calculated using a radiative transfer model. A short wave multi-stream model, using the discrete-ordinate method of Stamnes et al. (1988) is adopted. The radiative transfer model includes the radiative effects of aerosols, clouds, Rayleigh scattering, and absorption by gases. The calculations were performed at T42 horizontal resolution and in 40 vertical layers between the surface and 10 hPa. Meteorological data including cloud cover was the same as that used to drive the CTM. Aerosols had no influence on cloud formation in this study and as the radiative transfer calculation was performed off-line, there was no feed-back effect on the model meteorology. Aerosol optical properties of SOA are taken to be similar

ACPD
8, 18911–18936, 2008

to POA (Myhre et al., 2007), and the aerosol is assumed to be externally mixed. The radiative forcing calculations are performed as the difference in the irradiance at the top of the atmosphere between simulations for pre-industrial and present day model runs. A more detailed description of the radiative transfer model can be found in Myhre et al. (2002).

4 Results

4.1 The change in SOA production and burden

The annual global production and mean burden of SOA for the model runs is shown in Table 3. The increase in annual mean SOA burden between the pre-industrial run Pind_std and the present day run Pres_std was 59% (0.26 Tg). When all the emissions except POA and sulphur from biomass burning are held at pre-industrial levels (Pind_BBpres), an increase in the mean SOA burden of 16% (0.07 Tg) was calculated relative to Pind_std, and when the 1750 biomass burning emissions of POA and sulphur are used in the present day run (Pres_BBpind), an increase in the SOA burden of 34%, or 0.15 Tg, relative to Pind_std, was found. This indicates that up to 58% of the total pre-industrial to present day SOA increase was due to anthropogenic emissions from fossil fuel and bio fuel burning, and 27% was due to increases in POA and sulphate aerosol from biomass burning. The remaining 15% increase found between Pind_std and Pres_std can be explained by differences in the oxidant fields due to biomass burning emissions of NO_x and VOC, and by differences in the co-location of SOA forming species and POA available for partitioning.

The fact that emissions from fossil and bio fuel burning contribute around twice as much to the SOA increase as the biomass burning emissions can be explained by examining the increase in POA resulting from these processes. The change in POA emissions between 1750 and 2004 was greatest for emissions from fossil and bio fuels, (an increase of 12.54 Tg yr^{-1}), while emissions from biomass burning increased by

ACPD
8, 18911–18936, 2008

8.7 Tg yr^{-1}. As shown below, the most wide spread increases in SOA have occurred over industrialised areas, where the increase in abundance of pre-existing aerosol, upon which the SOA can partition, has been the greatest.

When partitioning to sulphate aerosol is not accounted for, the increase in SOA burden between pre-industrial and present day simulations is 0.17 Tg, or about 51%.

The distribution of the increases in SOA at the surface, and in the total column are shown in Fig. 1. In panel A, showing the difference between runs Pres_std and Pind_std, substantial increases can be seen both in the biomass burning regions of South America and southern Africa. Large increases are also obvious in South East Asia, as well as over the industrialised areas, such as Europe and the east coast of the USA. In the column values (panel E), the increase in SOA over the ocean, in the outflow from the USA, Africa and South America can be seen. In panels B and F, showing the increase in SOA when partitioning to ammonium sulphate aerosol was not allowed (Pres_nosul - Pind_nosul), the increases are lower, especially over industrialised areas. Particularly notable is the smaller increase in the column SOA values to the east of Europe and also on the east coast of North America. Panels C and G show the SOA increase when 2004 biomass burning emissions of POA and sulphur were included in the pre-industrial run (the difference between Pind_std and Pind_BBpres). Most of the increase in SOA over Indonesia, as well as over Africa and South America, which was seen in panels B and F, was due to larger biomass burning emissions.

Panels D and H show the difference between runs Pind_std and Pres_BBpind. Most of the increased SOA over the east coast of the USA, South East Asia and, in the total column, to the east of Europe, is reproduced here.

The increase in SOA did not occur uniformly throughout the atmospheric column, rather the largest increases were seen at the surface. Figure 2 shows the annual, zonal mean change in SOA concentration for the different model runs. Panel A shows the difference between Pres_std and Pind_std. Between these two runs, the largest increases in SOA were in the tropics and close to the surface, below 600 hPa. Increases higher in the atmosphere can also be seen, especially in the Northern Hemisphere,

ACPD
8, 18911–18936, 2008

where significant SOA increases are found even at polar latitudes. At high southern latitudes, the increase was very small, due to the lack of sources. Transport from lower latitudes at altitudes around 300 hPa appears less active than in the Northern Hemisphere. SOA increased slightly between the two runs in the lower troposphere at high northern latitudes. Panel B shows the difference between Pres_nosul and Pind_nosul. Here the situation is similar to panel A, with the largest SOA increase occurring in the tropics near the surface. However, there is less of an increase in SOA at the surface in the northern sub-tropics in panel B. The increase in SOA throughout the troposphere at northern midlatitudes was also greater in panel A than panel B.

Around the tropopause however, the abundance of SOA actually decreased in Pres_std compared to Pind_std. Additionally, the gas phase species which partition to form SOA are reduced in the upper troposphere in Pres_std compared to Pind_std (not shown). Compared to the pre-industrial atmosphere, with present day industrial emissions, concentrations of the oxidants O_3 and NO_3 are higher, while OH is lower in the global average, but higher near sources of anthropogenic emissions, which are often near sources of SOA precursors. This results in a shift in SOA precursor oxidation towards the surface. As the SOA precursors are less soluble than the oxidation products, greater oxidation near the surface leads to higher SOA concentrations near the surface, but lower SOA concentrations higher in the atmosphere, as the species are washed out. In the pre-industrial atmosphere, more of the SOA precursors are transported further up in the troposphere before they are oxidised. The actual SOA concentrations near the tropical tropopause are around a factor of 10–50 less than at the surface.

Changes in partitioning due to higher POA and sulphate aerosol masses in the present day atmosphere also affect the distribution of SOA.

Panel C shows the increase in SOA between Pind_std and Pind_BBpres. The reduction in SOA at high northern latitudes was due to the lower biomass burning emissions in the 2004 inventory (see also Fig. 1). Most of the tropical increase, both at the surface and higher in the troposphere are accounted for in this panel, and therefore result from

ACPD
8, 18911–18936, 2008

increased biomass burning emissions of POA and sulphur. In panel D, the increase in SOA due to industrial and fuel burning emissions is shown (the difference between run Pres_BBpind and Pind_std). This panel shows clearly that the peak in SOA values between 20° N and 40° N is a result of industrial activity. Further, most of the increase throughout the northern midlatitude troposphere is reproduced in panel D. The increase in SOA extends further south than in panel C, due to the more widespread emissions. The total increase in the high southern latitudes, seen in panel A, is a result of higher partitioning of semi-volatile species into the aerosol phase, when the biomass as well as fuel burning POA sources are included. Interestingly, most of the upper tropospheric SOA increase over the tropics appears to be a result of industrial or fuel burning emissions.

The 59% increase in the global annual mean SOA burden since pre-industrial times is significantly larger than values calculated in other recent studies, for example 25% (Tsigaridis et al., 2006) and 43% (Liao and Seinfeld, 2005), however, it is much lower than the estimates from earlier studies, for example 300% (Kanakidou et al., 2000) and 316% (Chung and Seinfeld, 2002). A SOA scheme similar to that of Liao and Seinfeld (2005) was used here, however, we found a much greater increase of the SOA burden relative to the POA burden.

SOA, POA and SO_4 production and burden from other studies are compared with the values calculated here, in Table 4. In Liao and Seinfeld (2005), the 43% increase in SOA was accompanied by an increase in POA by a factor of 13.2, in contrast, when only partitioning to organic aerosol was accounted for in the Oslo CTM2, SOA increased by 63%, as POA increased by a factor of about 2.8. The fractional increase in sulphate since pre-industrial times, in Tsigaridis et al. (2006), is slightly higher than in this work (a factor of 2.6 vs. the factor of 2.1 increase in this work), while the increase in POA is slightly lower (a factor of 2.2 vs. the factor 2.7 increase here). However, the absolute increase in POA between Pind_std and Pres_std was about 0.8 Tg, and the absolute increase in SOA was 0.26 Tg, while Tsigaridis et al. (2006) found a total increase in POA of 0.33 Tg and an increase in SOA of 0.16 Tg. Therefore, the in-

ACPD
8, 18911–18936, 2008

crease in SOA is higher in Tsigaridis et al. (2006) on a per-terragram of POA basis. The total changes in organic aerosol, between pre-industrial times and the present, are 1.27 Tg, 0.49 Tg, 1.22 Tg and 1.16 Tg in Liao and Seinfeld (2005), Tsigaridis et al. (2006), Chung and Seinfeld (2002) and Pres_std-Pind_std respectively, thus the total change in organic aerosol in this study is similar to that in other works. Interestingly, Tsigaridis et al. (2006) predicted SOA values to be larger than POA, both in preindustrial times and present, while Liao and Seinfeld (2005) found SOA burdens to be significantly larger than POA in pre-industrial times, and significantly lower than POA burdens in the present. In this work, and that of Chung and Seinfeld (2002), the global mean SOA burden is lower than the POA burden, both in pre-industrial times and the present.

4.2 The radiative forcing of changes in SOA burden

The increase in SOA since 1750 resulted in a global annual average radiative forcing of $-0.086\,W\,m^{-2}$, in run Pres_std, or about twice the the forcing due only to the increase in POA emitted by fossil fuel burning, ($-0.04\,W\,m^{-2}$) which was calculated with this model in a previous experiment (Schulz et al., 2006). It is also large in comparison with the best estimate from the IPCC AR4 of the radiative forcing for POA (Forster et al., 2007), which was -0.05 [± 0.05] $W\,m^{-2}$. Table 3 shows that the increase in SOA due to industrial and fuel burning emissions was about twice as large as that due to emissions of POA and sulphur from biomass burning; the radiative forcing caused by the SOA associated with the biomass burning emissions on the other hand (see Table 5), was only a little more than a third of that of the SOA associated with the industrial/fuel burning emissions ($-0.021\,W\,m^{-2}$ and $-0.056\,W\,m^{-2}$, respectively). For run Pres_nosul, the forcing was calculated as $-0.058\,W\,m^{-2}$, relative to Pind_nosul.

The distribution of the radiative forcing caused by the SOA increases is shown in Fig. 3. Generally, the radiative forcing is strong over areas with large emissions of SOA precursors or POA, and weak over remote ocean areas and at high latitudes.

Figure 3, panel A, shows the radiative forcing when SOA was also allowed to partition

ACPD
8, 18911–18936, 2008

to ammonium sulphate aerosol. Compared with panel D (no partitioning to sulphate), the forcing is much stronger over the industrialised areas, particularly to the east of Europe. There is also a large strengthening of the forcing on the East coast of the USA, and a weak forcing is seen to the east of the USA, over the ocean, as well as in the outflow to the west of Asia.

The forcing calculated from Pres_nosul (panel D) is mostly limited to the regions with high biomass burning emissions, as well as South East Asia, and over the ocean on the west coast of Africa.

Panel B and C show the forcing calculated from runs Pres_BBpind and Pind_BBpres respectively. The radiative forcing due to SOA partitioning to the increased levels of biomass burning POA is mainly evident over Southern Africa, Indonesia and South America, while the forcing resulting from the increased SOA due to industrial emissions occurred mainly over the industrial areas, as expected, considering the distribution of SOA increases shown in Fig. 1. It should be noted again, that the radiative forcing calculated here is the direct radiative forcing, and that the model does not account for indirect effects such as the influence of aerosol on cloud cover.

5 Discussion

The production of SOA was found to have increased by 28 Tg yr^{-1}, while the burden increased by 26 Tg, or 59%. The major part of this change was due to increases in industrial emissions, and the fact that the difference in SOA burden between Pres_std and Pres_nosul is a large fraction of the difference in burden between Pres_std and Pind_std suggests that the mass of aerosol available for partitioning may be the most significant cause of the increase in SOA. Most of the upper tropospheric SOA increase over the tropics appears not to be a result of increases in biomass burning emissions of POA or sulphur, rather due to industrial or fuel burning emissions.

The results also suggest that although the global burden of SOA has increased since pre-industrial times, the concentrations of SOA in the upper troposphere have

ACPD
8, 18911–18936, 2008

decreased. This is due to changes in the altitudes and locations at which oxidation and partitioning of SOA species occur, which in turn affects the removal of the organic species from the atmosphere.

The radiative forcing resulting from SOA is $-0.09\,\mathrm{Wm}^{-2}$, for Pres_std, compared to Pind_std. The radiative forcing modelled here is likely to be slightly weaker than the actual radiative forcing, due to the importance of the total OA burden for SOA partitioning, and the fact that in industrialised regions the model tends to underestimate the concentrations of OA (Hoyle et al., 2007).

Observations show a large fraction of OA to be secondary in origin (Crosier et al., 2007; Gelencser et al., 2007), and there are indications that anthropogenic VOC, or processing by anthropogenically influenced air masses, could be more important for SOA formation than the current state-of-the-art SOA models predict (Volkamer et al., 2006; Crosier et al., 2007). Therefore, further characterisation of the anthropogeic effect on SOA formation is necessary to improve model results near industrialised areas.

If the work of Lelieveld et al. (2008) is confirmed, the development of a parameterisation for the recycling of OH during isoprene oxidation would be a substantial improvement to the chemistry leading to SOA formation. Such a mechanism would lead to higher SOA yields in areas with significant isoprene emissions, and may lead to a better match between modelled and measured OA values.

A further factor that may help improve the modelled mass of SOA, is the measurement of SOA yields in the laboratory, at an atmospherically relevant range of temperatures. This would reduce the reliance on the extrapolation of partitioning coefficients from a single temperature, using a generalised enthalpy of vaporisation.

The inclusion of sulphate aerosol as mass to which SOA can partition caused large increases in the amount of SOA in and near large industrial agglomerations. Regulations which lead to further reductions in emissions of sulphur may therefore lead to lower burdens of organic aerosol in, and down-wind of these areas. In order to model the effects of such reductions, however, the representation of sulphate aerosol and its interaction with organics in large scale models needs to be improved. Water

uptake, as well as deliquescence and efflorescence of ammonium sulphate needs to be accounted for, as both these factors influence the uptake of semi-volatile organic species. This will be the focus of future work with this model.

Acknowledgements. This work was carried out with funding from the projects BACCI (Biosphere-Aerosol-Cloud-Climate Interactions) and EUCAARI (European Integrated project on Aerosol Cloud Climate and Air Quality Interactions).

References

Berglen, T. F., Berntsen, T. K., Isaksen, I. S. A., and Sundet, J. K.: A global model of the coupled sulfur/oxidant chemistry in the troposphere: The sulfur cycle, J. Geophys. Res., 109, D19310, doi:10.1029/2003JD003948, 2004. 18914

Berntsen, T. K. and Isaksen, I. S. A.: A global three-dimensional chemical transport model for the troposphere 1. Model description and CO and ozone results, J. Geophys. Res., 102, 21 239–21 280, doi:10.1029/97JD01140, 1997. 18914

Bond, T. C., Streets, D. G., Yarber, K. F., Nelson, S. M., Woo, J.-H., and Klimont, Z.: A technology-based global inventory of black and organic carbon emissions from combustion, J. Geophys. Res.-Atmos., 109, D14203, doi:10.1029/2003JD003697, 2004. 18917

Chung, S. H. and Seinfeld, J. H.: Global distribution and climate forcing of carbonaceous aerosols, J. Geophys. Res.-Atmos., 107, 4407, doi:10.1029/2001JD001397, 2002. 18913, 18921, 18922, 18932

Crosier, J., Allan, J. D., Coe, H., Bower, K. N., Formenti, P., and Williams, P. I.: Chemical composition of summertime aerosol in the Po Valley (Italy), northern Adriatic and Black Sea, Q. J. Roy. Meteor. Soc., 133, 61–75, doi:10.1002/qj.88, 2007. 18924

Dentener, F., Kinne, S., Bond, T., Boucher, O., Cofala, J., Generoso, S., Ginoux, P., Gong, S., Hoelzemann, J. J., Ito, A., Marelli, L., Penner, J. E., Putaud, J.-P., Textor, C., Schulz, M., van der Werf, G. R., and Wilson, J.: Emissions of primary aerosol and precursor gases in the years 2000 and 1750 prescribed data-sets for AeroCom, Atmos. Chem. Phys., 6, 4321–4344, 2006, http://www.atmos-chem-phys.net/6/4321/2006/. 18917

Forster, P., Ramaswamy, V., Artaxo, P., Berntsen, T., Betts, R., Fahey, D., Haywood, J., Lean, J., Lowe, D., Myhre, G., Nganga, J., Prinn, R., Raga, G., Schulz, M., and Van Dorland,

R.: Climate Change 2007: The Physical Science Basis. Contribution of Working Group I to the Fourth Assessment Report of the Intergovernmental Panel on Climate Change, Chap. 2, Changes in Atmospheric Constituents and in Radiative Forcing, Cambridge University Press, Cambridge, United Kingdom and New York, NY, USA, 2007. 18922

Gelencser, A., May, B., Simpson, D., Sanchez-Ochoa, A., Kasper-Giebl, A., Puxbaum, H., Caseiro, A., Pio, C., and Legrand, M.: Source apportionment of PM2.5 organic aerosol over Europe: Primary/secondary, natural/anthropogenic, and fossil/biogenic origin, J. Geophys. Res.-Atmos., 112, D23S04, doi:10.1029/2006JD008094, 2007. 18924

Granier, C., Lamarque, J. F., Mieville, A., Muller, J. F., Olivier, J., Orlando, J., Peters, J., Petron, G., Tyndall, G., and Wallens, S.: POET, a database of surface emissions of ozone precursors, available online: http://www.aero.jussieu.fr/projet/ACCENT/POET.php, 2005. 18916

Guenther, A., Hewitt, C. N., Erickson, D., Fall, R., Geron, C., Graedel, T., Harley, P., Klinger, L., Lerdau, M., McKay, W. A., Pierce, T., Scholes, B., Steinbrecher, R., Tallamraju, R., Taylor, J., and Zimmerman, P.: A global model of natural volatile organic compound emissions, J. Geophys. Res., 100, 8873–8892, doi:10.1029/94JD02950, 1995. 18916

Guenther, A., Karl, T., Harley, P., Wiedinmyer, C., Palmer, P. I., and Geron, C.: Estimates of global terrestrial isoprene emissions using MEGAN (Model of Emissions of Gases and Aerosols from Nature), Atmos. Chem. Phys., 6, 3181–3210, 2006, http://www.atmos-chem-phys.net/6/3181/2006/. 18916

Henze, D. K. and Seinfeld, J. H.: Global secondary organic aerosol from isoprene oxidation, Geophys. Res. Lett., 33, L09812, doi:10.1029/2006GL025976, 2006. 18913

Hesstvedt, E., Hov, Ø., and Isaksen, I. S. A.: Quasi-Steady-State Approximations in Air-Pollution Modeling – Comparison of Two Numerical Schemes for Oxidant Prediction, Int. J. Chem. Kinet., 10, 971–994, 1978. 18914

Hoyle, C. R., Berntsen, T., Myhre, G., and Isaksen, I. S. A.: Secondary organic aerosol in the global aerosol – chemical transport model Oslo CTM2, Atmos. Chem. Phys., 7, 5675–5694, 2007, http://www.atmos-chem-phys.net/7/5675/2007/. 18915, 18924

IPCC: Climate Change 2001: The Scientific Basis. Contribution of Working Group I to the Third Assessment Report of the Intergovernmental Panel on Climate Change, Cambridge University Press, Cambridge, United Kingdom and New York, NY, USA, 881 pp., 2001. 18916

IPCC: Climate Change 2007: Synthesis Report. Contribution of Working Groups I II and III to the Fourth Assessment Report of the Intergovernmental Panel on Climate Change, IPCC,

Geneva, Switzerland, 104 pp., 2007. 18912
Kanakidou, M., Tsigaridis, K., Dentener, F. J., and Crutzen, P. J.: Human-activity-enhanced formation of organic aerosols by biogenic hydrocarbon oxidation, J. Geophys. Res., 105, 9243–9254, doi:10.1029/1999JD901148, 2000. 18913, 18921
Kanakidou, M., Seinfeld, J. H., Pandis, S. N., Barnes, I., Dentener, F. J., Facchini, M. C., Van Dingenen, R., Ervens, B., Nenes, A., Nielsen, C. J., Swietlicki, E., Putaud, J. P., Balkanski, Y., Fuzzi, S., Horth, J., Moortgat, G. K., Winterhalter, R., Myhre, C. E. L., Tsigaridis, K., Vignati, E., Stephanou, E. G., and Wilson, J.: Organic aerosol and global climate modelling: a review, Atmos. Chem. Phys., 5, 1053–1123, 2005, http://www.atmos-chem-phys.net/5/1053/2005/. 18912
Kaufman, Y., Tanre, D., and Boucher, O.: A satellite view of aerosols in the climate system, Nature, 419, 215–223, doi:10.1038/nature01091, 2002. 18912
Lathière, J., Hauglustaine, D. A., De Noblet-Ducoudré, N., Krinner, G., and Folberth, G. A.: Past and future changes in biogenic volatile organic compound emissions simulated with a global dynamic vegetation model, Geophys. Res. Lett., 32, L20818, doi:10.1029/2005GL024164, 2005. 18916
Lathière, J., Hauglustaine, D. A., Friend, A. D., De Noblet-Ducoudré, N., Viovy, N., and Folberth, G. A.: Impact of climate variability and land use changes on global biogenic volatile organic compound emissions, Atmos. Chem. Phys., 6, 2129–2146, 2006, http://www.atmos-chem-phys.net/6/2129/2006/. 18916
Lelieveld, J., Butler, T. M., Crowley, J. N., Dillon, T. J., Fischer, H., Ganzeveld, L., Harder, H., Lawrence, M. G., Martinez, M., Taraborrelli, D., and Williams, J.: Atmospheric oxidation capacity sustained by a tropical forest, Nature, 452, 737–740, doi:10.1038/nature06870, 2008. 18916, 18924
Liao, H. and Seinfeld, J. H.: Global impacts of gas-phase chemistry-aerosol interactions on direct radiative forcing by anthropogenic aerosols and ozone, J. Geophys. Res.-Atmos., 110, D18208, doi:10.1029/2005JD005907, 2005. 18913, 18921, 18922, 18932
Müller, J.-F., Stavrakou, T., Wallens, S., De Smedt, I., Van Roozendael, M., Potosnak, M. J., Rinne, J., Munger, B., Goldstein, A., and Guenther, A. B.: Global isoprene emissions estimated using MEGAN, ECMWF analyses and a detailed canopy environment model, Atmos. Chem. Phys., 8, 1329–1341, 2008, http://www.atmos-chem-phys.net/8/1329/2008/. 18916
Myhre, G., Jonson, J. E., Bartnicki, J., Stordal, F., and Shine, K. P.: Role of spatial and temporal

variations in the computation of radiative forcing due to sulphate aerosols: A regional study, Q. J. Roy. Meteor. Soc., 128, 973–989, 2002. 18918

Myhre, G., Bellouin, N., Berglen, T. F., Berntsen, T. K., Boucher, O., Grini, A., Isaksen, I. S. A., Johnsrud, M., Mishchenko, M. I., Stordal, F., and Tanré, D.: Comparison of the radiative properties and direct radiative effect of aerosols from a global aerosol model and remote sensing data over ocean, Tellus B, 59, 115–129, doi:10.1111/j.1600-0889.2006.00226.x, 2007. 18918

Odum, J. R., Hoffmann, T., Bowman, F., Collins, D., Flagan, R. C., and Seinfeld, J. H.: Gas/Particle Partitioning and Secondary Organic Aerosol Yields, Environ. Sci. Technol., 30, 2580–2585, 1996. 18914

Schulz, M., Textor, C., Kinne, S., Balkanski, Y., Bauer, S., Berntsen, T., Berglen, T., Boucher, O., Dentener, F., Guibert, S., Isaksen, I. S. A., Iversen, T., Koch, D., Kirkevåg, A., Liu, X., Montanaro, V., Myhre, G., Penner, J. E., Pitari, G., Reddy, S., Seland, Ø., Stier, P., and Takemura, T.: Radiative forcing by aerosols as derived from the AeroCom present-day and pre-industrial simulations, Atmos. Chem. Phys., 6, 5225–5246, 2006, http://www.atmos-chem-phys.net/6/5225/2006/. 18912, 18922

Stamnes, K., Tsay, S.-C., Jayaweera, K., and Wiscombe, W.: Numerically stable algorithm for discrete-ordinate-method radiative transfer in multiple scattering and emitting layered media, Appl. Opt., 27, 2502–2509, 1988. 18917

Tsigaridis, K., Krol, M., Dentener, F. J., Balkanski, Y., Lathière, J., Metzger, S., Hauglustaine, D. A., and Kanakidou, M.: Change in global aerosol composition since preindustrial times, Atmos. Chem. Phys., 6, 5143–5162, 2006, http://www.atmos-chem-phys.net/6/5143/2006/. 18913, 18921, 18922, 18932

van der Werf, G. R., Randerson, J. T., Giglio, L., Collatz, G. J., Kasibhatla, P. S., and Arellano Jr., A. F.: Interannual variability in global biomass burning emissions from 1997 to 2004, Atmos. Chem. Phys., 6, 3423–3441, 2006, http://www.atmos-chem-phys.net/6/3423/2006/. 18917

Volkamer, R., Jimenez, J. L., San Martini, F., Dzepina, K., Zhang, Q., Salcedo, D., Molina, L. T., Worsnop, D. R., and Molina, M. J.: Secondary organic aerosol formation from anthropogenic air pollution: Rapid and higher than expected, Geophys. Res. Lett., 33, L17811, doi:10.1029/2006GL026899, 2006. 18924

Table 1. The model experiments which were carried out. The year used for the biomass burning emissions of POA (and sulphur, where relevant) is given in the column "BB year". The year used for all other emissions is given in the column "Emis. year". The entries in the column "Sulph." indicate whether or not SOA was allowed to partition to sulphate aerosol.

Name	Emis. year	BB year	Sulph.
Pind_std	1750	1750	YES
Pres_std	2004	2004	YES
Pres_BBpind	2004	1750	YES
Pind_BBpres	1750	2004	YES
Pind_nosul	1750	1750	NO
Pres_nosul	2004	2004	NO

ACPD
8, 18911–18936, 2008

Table 2. The emissions used in the model runs. BVOC includes the total emissions of biogenic volatile organic carbon, which can react to form SOA. AVOC is the anthropogenic equivalent. References for the emission data sets are provided in the text.

run	Emissions					
	CO	NO_x	POA	BVOC	AVOC	isoprene
1750BS	343 Tg yr^{-1}	11.4 Tg (N) yr^{-1}	10.26 Tg (C) yr^{-1}	386 Tg (C) yr^{-1}	1.21 Tg yr^{-1}	220 Tg yr^{-1}
2004BS	1061 Tg yr^{-1}	46.7 Tg (N) yr^{-1}	30.40 Tg (C) yr^{-1}	386 Tg (C) yr^{-1}	21.62 Tg yr^{-1}	220 Tg yr^{-1}
2004–1750 BB	1061 Tg yr^{-1}	46.7 Tg (N) yr^{-1}	18.04 Tg (C) yr^{-1}	386 Tg (C) yr^{-1}	21.62 Tg yr^{-1}	220 Tg yr^{-1}
1750–2004 BB	343 Tg yr^{-1}	11.4 Tg (N) yr^{-1}	22.62 Tg (C) yr^{-1}	386 Tg (C) yr^{-1}	1.21 Tg yr^{-1}	220 Tg yr^{-1}
1750B	343 Tg yr^{-1}	11.4 Tg (N) yr^{-1}	10.26 Tg (C) yr^{-1}	386 Tg (C) yr^{-1}	1.21 Tg yr^{-1}	220 Tg yr^{-1}
2004B	1061 Tg yr^{-1}	46.7 Tg (N) yr^{-1}	30.40 Tg (C) yr^{-1}	386 Tg (C) yr^{-1}	21.62 Tg yr^{-1}	220 Tg yr^{-1}

ACPD
8, 18911–18936, 2008

Table 3. Global, annual mean SOA production and burden for the various model runs.

Run	Production (Tg yr^{-1})	Burden (Tg)
Pind_std	42.8	0.44
Pind_nosul	34.5	0.33
Pres_std	68.8	0.70
Pres_nosul	53.4	0.50
Pind_BBpres	47.0	0.51
Pres_BBpind	62.4	0.59

ACPD
8, 18911–18936, 2008

Table 4. A comparison between aerosol burdens in this, and similar studies. Values are given for pre-industrial model runs, present day model runs and the fraction change between the two. The units are Tg.

Model study	Species	pre-ind.	Pres.	fraction change
Liao and Seinfeld (2005)	SO_4	0.32	1.4	4.38
	POA	0.10	1.27	13.2
	SOA	0.23	0.33	1.43
Tsigaridis et al. (2006)	SO_4	0.4	1.05	2.6
	POA	0.27	0.6	2.2
	SOA	0.64	0.8	1.25
This work (std)	SO_4	0.84	1.80	2.14
	POA	0.51	1.41	2.78
	SOA	0.44	0.7	1.59
This work (nosul)	POA	0.51	1.41	2.78
	SOA	0.32	0.52	1.63
Chung and Seinfeld (2002)	POA	0.11	1.2	10.91
	SOA	0.06	0.19	3.17

ACPD
8, 18911–18936, 2008

Table 5. The radiative forcing as a result of SOA increases since pre-industrial times, for the different model runs.

Run	RF ($W m^{-2}$)
Pind_std/Pres_std	−0.086
Pind_nosul/Pres_nosul	−0.058
Pind_BBpres/Pind_std	−0.021
Pres_BBpind/Pind_std	−0.056

ACPD
8, 18911–18936, 2008

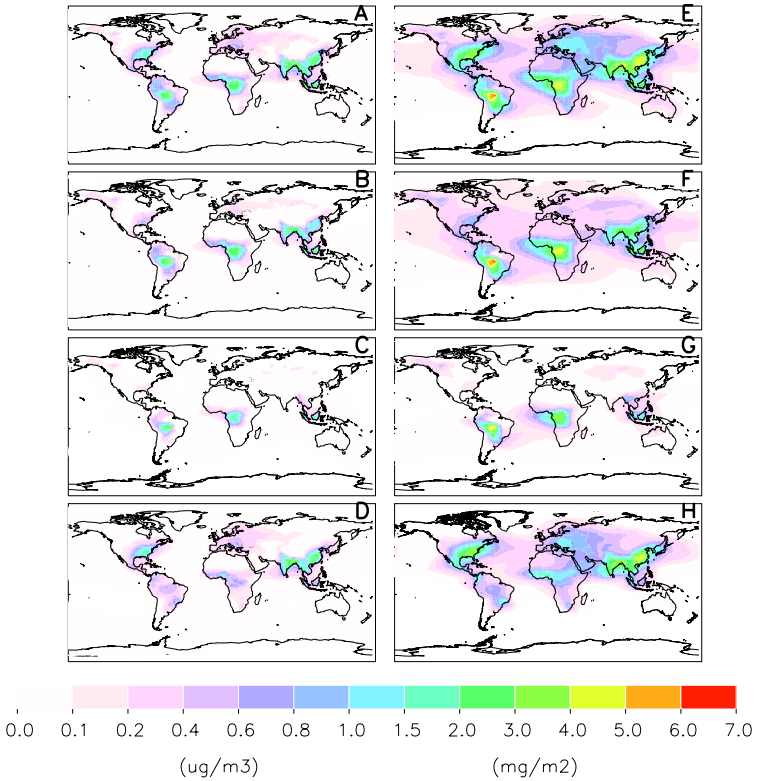

Fig. 1. The increase in annual mean SOA concentration since pre-industrial times. Panels **(A–D)** show changes at the surface, panels **(E–H)** show changes for the total column amount of SOA. Panels (A) and (E) show the difference between runs Pres_std and Pind_std, panels (B) and (F) show the difference between runs Pres_nosul and Pind_nosul, panels (C) and (G) show the difference between runs Pind_BBpres and Pind_std, and panels (D) and (H) show the difference between runs Pres_BBpind and Pind_std.

ACPD
8, 18911–18936, 2008

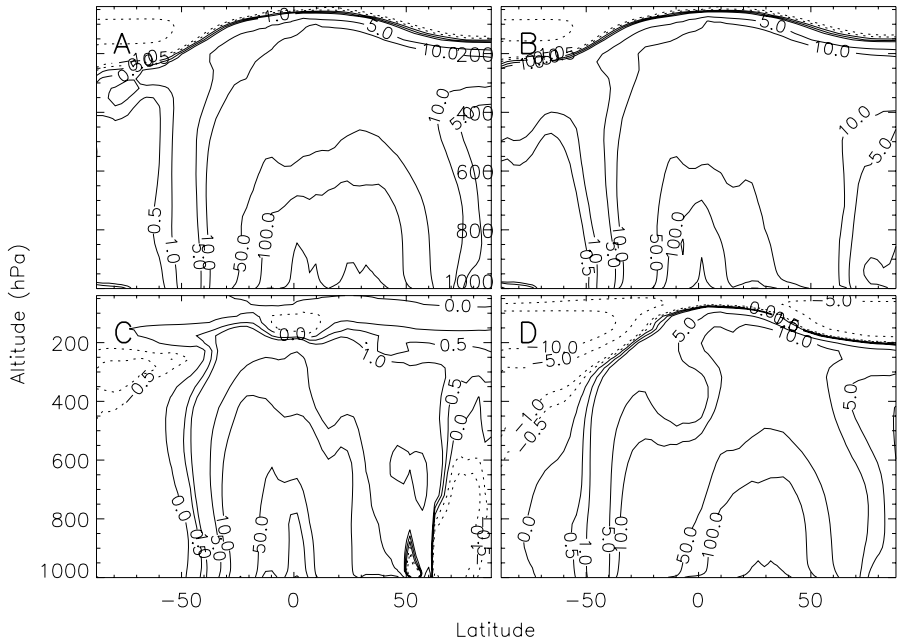

Fig. 2. The annual, zonal mean increase in SOA between the pre-industrial model runs and the present day runs (ng m^{-3}). Panel **(A)** shows the difference between Pres_std and Pind_std, panel **(B)** the difference between Pres_nosul and Pind_nosul, panel **(C)** the difference between Pind_BBpres and Pind_std, and panel **(D)** shows the difference between Pres_BBpind and Pind_std. The highest isoline in panels (A) and (D) is 200 ng m^{-3}.

ACPD
8, 18911–18936, 2008

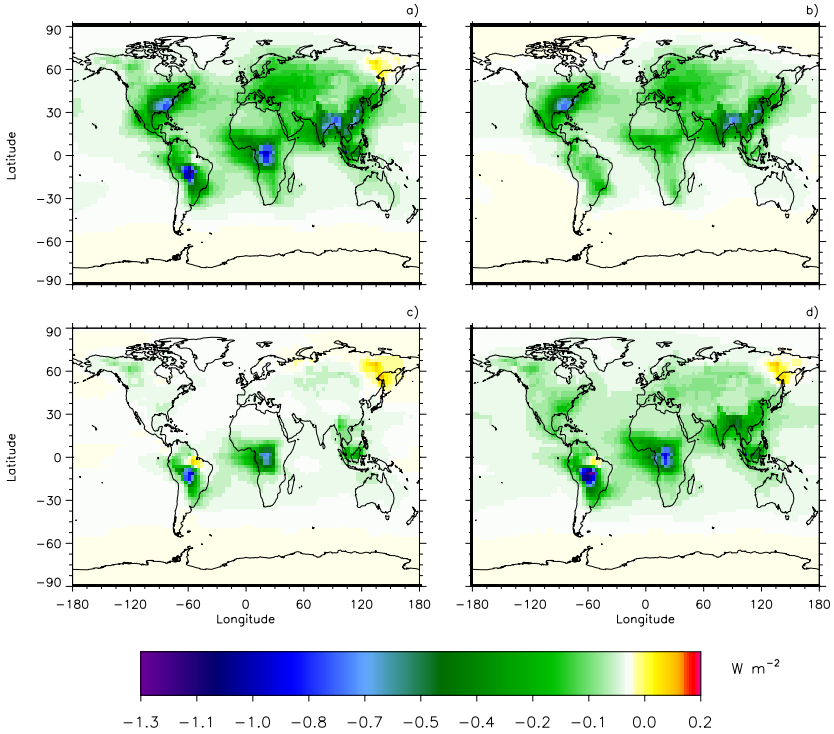

Fig. 3. The radiative forcing (RF) due to SOA increases between pre-industrial times and the present. Panel **(A)**: SOA is allowed to partition to POA and sulphate aerosol from all sources (calculated from Pind_std vs. Pres_std). Panel **(B)**: same as panel (A), but emissions of POA from biomass burning are set to pre-industrial values in the present day run (RF is calculated from Pind_std vs. Pres_BBpind). Panel **(C)**: RF is calculated from Pind_std vs. Pind_BBpres, i.e. the RF results from the increase in SOA due to biomass burning POA and sulphate aerosol. Panel **(D)** shows the RF when SOA is not allowed to partition to sulphate aerosol (Pind_nosul vs. Pres_nosul)

ACPD
8, 18911–18936, 2008